

## EFFECT OF LIQUID PHASE COMPRESSIBILITY ON MODELLING OF GAS-LIQUID TWO-PHASE FLOWS USING TWO-FLUID MODEL

by

**Vahid SHOKRI\* and Kazem ESMAEILI**

Department of Mechanical Engineering, Sari Branch, Islamic Azad University, Sari, Iran

Original scientific paper

<https://doi.org/10.2298/TSCI171018148S>

*In this paper, a numerical study is performed in order to investigate the effect of the liquid phase compressibility two-fluid model. The two-fluid model is solved by using conservative shock capturing method. At the first, the two-fluid model is applied by assuming that the liquid phase is incompressible, then it is assumed that in three cases called water faucet case, large relative velocity shock pipe case, and Toumi's shock pipe case, the liquid phase is compressible. Numerical results indicate that, if an intense pressure gradient is governed on the fluid-flow, single-pressure two-fluid model by assuming liquid phase incompressibility predicts the flow variables in the solution field more accurate than single-pressure two-fluid model by assuming liquid phase compressibility.*

Key words: *two-phase flow, two-fluid model, phase compressible, numerical simulation*

### Introduction

Two-phase flows are important in many applications such as oil and gas industries, nuclear power plants, thermal power plants, petrochemical industries, and oil and gas transmission from Oilfield. Therefore, more accurate prediction of two-phase flows within the transfer pipe-lines is essential. Applying the proper mathematical model is one of the most important parameters in numerical modelling of two-phase flows. According to Eulerian approach, mathematical modelling of two-phase flows are categorized homogeneous equilibrium model [1], drift-flux model [2], and multi-phase flow model [3].

In this study, we focus on the two-fluid model. The two-fluid model consists of two sets of conservation equations for the balance of mass, momentum, and energy for each phase. For using two-fluid model and completing equations, we require suitable closure model and appropriate assumptions for phase pressures, phase temperatures, phase compressibility, and mass transfer between phases. The purpose of this study is to investigate the effect of assuming liquid phase compressibility in the two-fluid model and its effect on the accuracy of the obtained numerical results. Two forms of the two-fluid model are presented in order to analyze isotherm compressible two-phase flows single-pressure two-fluid model [4] and two-pressure two-fluid model [5-7].

Cortes *et al.* [8], for solving two-fluid model equations, they assumed that liquid phase pressure is equal to gas phase pressure, also they assumed that the liquid phase is incompressible and the gas phase is perfect gas for the vapor phase. Song and Ishii [9], studied well-posedness

\* Corresponding author, e-mail: shokri.vhd@iausari.ac.ir

of the incompressible 1-D two-fluid model. In their work, gas phase pressure and liquid phase pressure is considered the same as well as gas phase and liquid phase are considered as incompressible. Evje and Flatten [10], used hybrid flux splitting schemes in order to solve the single-pressure two-fluid model. In their work, the liquid phase density and the gas phase density was assumed variable in order to apply hybrid flux splitting schemes.

Issa and Kempf [11], in order to the simulation of slug flow in horizontal and nearly horizontal pipes with the two-fluid model, used the single-pressure two-fluid model by assuming gas phase compressibility and liquid phase incompressibility. In their model, they considered that the gas phase pressure at the interface is equal to the liquid phase pressure at the interface as well as they assumed that liquid phase pressure in the vertical direction is hydrostatic. Omgba-Essama [1], used the Issa and Kemp's [11] assumptions of pressure in order to numerical modelling two-phase two-fluid-flows. He considered gas phase compressibility and liquid phase incompressibility and modeled numerically central formulation based on Riemann Solver.

Liao *et al.* [12], considered the numerical stability of two-fluid model near to ill-posedness condition by considering incompressibility of the gas and liquid phases. In their study, they used the Issa and Kemp's [11] pressure assumptions but the difference is that, in their model, they neglected pressure correction term in the gas phase. Issa *et al.* [13], used the two-fluid model in order to improve closure models for gas entrainment and interfacial shear for slug flow modelling in horizontal pipes. they also used the Issa and Kemp's [11] assumptions of pressure by considering the of the liquid phase incompressibility and the gas phase compressibility. They also applied the ideal gas relationship in order to its calculation.

Hanyang and Liejin [14] and Ansari and Shokri [15], used the transient two-fluid model in order to numerical modelling of stratified gas-liquid two-phase flow. They considered gas phase and liquid phase as incompressible. Holmas *et al.* [16] conducted a study on analysis of a 1-D incompressible two-fluid model including artificial diffusion. Holmas [17] used the two-fluid model in order to the numerical simulation of transient roll-waves in two-phase pipe flow, by assuming incompressibility of phases. Ansari and Shokri [18], used the incompressibility of phases assumption in order to numerical modelling of slug flow initiation in horizontal channels using a two-fluid model.

Ansari and Daramizadeh [19] conducted a study titled *Slug type hydrodynamic instability analysis using a five equations hyperbolic two-pressure, two-fluid model*. In their work on the two-fluid model, they considered gas phase and liquid phase as compressible. Using two-fluid, comparison of implicit and explicit AUSM-family schemes for compressible multiphase flows was performed [20]. Shokri and Esmaeili [21] compared the effect of hydrodynamic and hydrostatic models for pressure correction term in the single-pressure two-fluid model. The two-fluid model was solved by assuming gas phase compressibility and liquid phase incompressibility.

In the numerical solution of two-phase flows due to the existence of deformable interface, fluid properties vary discontinuously across this interface. It is very important to select a suitable model in order to predict such discontinuities during passing through the interface. According to the literature review, it was found that single-pressure two-fluid model is presented in two forms in the literature. In the first form, the liquid phase is assumed as incompressible and in the second form, the liquid phase is assumed as compressible. Also, according to the literature review, there was no comparison of the single-pressure two-fluid model with the assumption of the liquid phase compressibility and the single-pressure two-fluid model with the assumption of the gas phase incompressibility. Therefore, innovation of the present study is to compare the single-pressure two-fluid model with the assumption of the liquid phase

compressibility and the single-pressure two-fluid model with the assumption of the gas phase incompressibility.

### Two-fluid model

The two-fluid model is formulated based on two conservation equations for mass and momentum balance for the two fluids (*i. e.* gas and liquid). The model is considered as isotropic and also energy equation is neglected. In this section, governing equations on the two-fluid model are presented. In this work, the governing assumptions are:

- the effects of the friction between wall and phases and the friction at the interface are neglected,
- the only body force is gravitational force, and
- mass transfer between the two-phases is neglected,

The governing equations on the single-pressure are included two continuity equations and two momentum equations [10]. The equations of the single-pressure model are presented as below.

- Gas and liquid continuity equations:

$$\frac{\partial}{\partial t}(\rho_g R_g) + \frac{\partial}{\partial x}(\rho_g R_g u_g) = 0 \quad (1)$$

$$\frac{\partial}{\partial t}(\rho_l R_l) + \frac{\partial}{\partial x}(\rho_l R_l u_l) = 0 \quad (2)$$

- Gas and liquid momentum equations:

$$\frac{\partial}{\partial t}(\rho_g R_g u_g) + \frac{\partial}{\partial x}(\rho_g R_g u_g^2) = -\frac{\partial}{\partial x}[(P_g - P_{gi})R_g] - R_g \frac{\partial P_{gi}}{\partial x} - \rho_g R_g g \sin \beta \quad (3)$$

$$\frac{\partial}{\partial t}(\rho_l R_l u_l) + \frac{\partial}{\partial x}(\rho_l R_l u_l^2) = -\frac{\partial}{\partial x}[(P_l - P_{li})R_l] - R_l \frac{\partial P_{li}}{\partial x} - \rho_l R_l g \sin \beta \quad (4)$$

where for  $k^{th}$  phase ( $k = g$  then the phase is gas and if  $k = l$  the phase is liquid),  $\rho_k$  – the density of  $k^{th}$  phase,  $R_k$  – the volume fraction of  $k^{th}$  phase,  $u_k$  – the velocity of  $k^{th}$  phase,  $P_k$  – the pressure of  $k^{th}$  phase,  $P_{ki}$  – the pressure of  $k^{th}$  phase at the interface,  $\beta$  – the inclination of the pipe, and  $g$  – the acceleration of gravity. In the present model, gas is equal to liquid pressure (*i. e.*  $P_g = P_l = P$ ) as well as the pressure of phases at the interface are the same (*i. e.*  $P_{gi} = P_{li} = P_i$ ). Thus, eqs. (3) and (4) are re-written:

$$\frac{\partial}{\partial t}(\rho_g R_g u_g) + \frac{\partial}{\partial x}(\rho_g R_g u_g^2 + R_g P) = P_i \frac{\partial R_g}{\partial x} - \rho_g R_g g \sin \beta \quad (5)$$

$$\frac{\partial}{\partial t}(\rho_l R_l u_l) + \frac{\partial}{\partial x}(\rho_l R_l u_l^2 + R_l P) = P_i \frac{\partial R_l}{\partial x} - \rho_l R_l g \sin \beta \quad (6)$$

In momentum equations, the term is shown as and called *correction pressure term*. the following relation is presented in order to calculate this term [8, 22]:

$$\Delta P_{ki} = P_k - P_{ki} = \delta \frac{R_l R_g \rho_l \rho_g}{\rho_g R_l + \rho_l R_g} (u_g - u_l)^2 \quad (7)$$

where  $\delta = 1.2$  [10] for closing equation system, additional equations are required. The first equation is a geometric constraint. It states that summation of the volume fraction of the two-phases is equal to unit. The constraint equation of gas-liquid mixture [23]:

$$R_l + R_g = 1 \quad (8)$$

In addition the eq. (8), thermodynamics sub-models is required. For  $k^{th}$  phase, the following linear equation is considered in order to express the relationship between density and pressure [24]:

$$\rho_k = \rho_{0,k} + \frac{P - P_{0,k}}{C_k^2} \quad (9)$$

and are given reference value for density and pressure, respectively. is the speed of sound in every phase [25]:

$$\frac{\partial P_k}{\partial \rho_k} = C_k^2 \quad (10)$$

The gas sound speed and the gas reference value density and gas reference value pressure are presented  $(10^5)^{1/2}$  [ $\text{ms}^{-1}$ ], 0, and 0, respectively, [10]. The liquid sound speed and the liquid reference value density and liquid reference value pressure are presented  $10^3$  [ $\text{ms}^{-1}$ ],  $10^3$  [ $\text{kgm}^{-3}$ ], and  $10^5$  [Pa], respectively, [10].

#### *Instantaneous pressure relaxation method*

In order to consider liquid phase compressibility, another equation is required for equaling the number of equations to the number of unknowns. Evje and Flatten [10], considered liquid phase compressibility using instantaneous pressure relaxation method. In the instantaneous pressure relaxation method, gas phase pressure and liquid phase pressure are considered as the same, therefore, this is similar to the assumptions of single-pressure two-fluid model pressure. Evje and Flatten [10], presented the eq. (11) for instantaneous pressure relaxation:

$$\frac{R_g \rho_g}{\rho_{g(P)}} + \frac{R_l \rho_l}{\rho_{l(P)}} = 1 \quad (11)$$

Instead of the denominator densities, the eq. (9) is substituted and finally, the following quadratic equation is obtained in order to calculate pressure term. The pressure is obtained by solving the above quadratic eq. (12):

$$P^2 + P \left[ C_l^2 (\rho_{0,l} - R_l \rho_l) + C_g^2 (\rho_{0,g} - R_g \rho_g) - (P_{0,l} + P_{0,g}) \right] - C_g^2 C_l^2 \cdot \\ \cdot (R_g \rho_g \rho_{0,l} + R_l \rho_l \rho_{0,g} - \rho_{0,g} \rho_{0,l}) - C_g^2 P_{0,l} (\rho_{0,g} - R_g \rho_g) - C_l^2 P_{0,g} (\rho_{0,l} - R_l \rho_l) + P_{0,g} P_{0,l} = 0 \quad (12)$$

#### **Numerical method for solving equation**

Non-conservative Single-pressure two-fluid model is written [26]:

$$\frac{\partial Q}{\partial t} + \frac{\partial F}{\partial x} = H \frac{\partial R_k}{\partial x} + S \quad (13)$$

where  $Q$  is conservative variables vector,  $F$  – the conservative flux vector. The vectors  $S$  and  $H$  are source term vector and interfacial pressure vectors, respectively. For the non-conservative system eq. (13), discretization form of the equation is expressed [26]:

$$Q_i^{n+1} = Q_i^n + \frac{\Delta t}{\Delta x} (F_{i-1/2}^{n\text{Force}} - F_{i+1/2}^{n\text{Force}}) + \Delta t \left( H \frac{\partial R_k}{\partial x} \right) + \Delta t S_i \quad (14)$$

In the eq. (14),  $n$  and  $n + 1$  show old-time step and new time step, respectively. Also  $i$  is the cell. In order to calculate the numerical flux term  $F_{i+1/2}^{n\text{Force}}$ , force method is used [26]:

$$F_{i+1/2}^{nForce} = \frac{1}{2} (F_{i+1/2}^{nLF} + F_{i+1/2}^{nRI}) \quad (15)$$

The  $F_{i+1/2}^{nLF}$  is the Lax-Friedrichs numerical flux and  $F_{i+1/2}^{nRI}$  – the Ritzhmyer numerical flux. In the Lax-Friedrichs method, flux term is calculated [26, 27]:

$$F_{i+1/2}^{nLF} = \frac{1}{2} (F_{i+1}^n + F_i^n) - \frac{\Delta x}{2\Delta t} (Q_{i+1}^n - Q_i^n) \quad (16)$$

In the Ritzhmyer method, flux term is calculated [27]:

$$F_{i+1/2}^{nRI} = F(Q_{i+1/2}^{n+1/2}) \quad (17)$$

$$Q_{i+1/2}^{n+1/2} = \frac{1}{2} (Q_i^n + Q_{i+1}^n) - \frac{\Delta t}{2\Delta x} (F_i^n - F_{i+1}^n) \quad (18)$$

Numerical flux in the  $i^{th}$  cell is defined as  $F_i^n = F(Q_i^n)$  and obtained according to physical flux term that is stated by the model. Two-fluid equations have the non-conservative terms ( $H\partial R_k/\partial x$ ) that must be discretized well. Lock of properly discretizing of this term leads to instability in results [28]. For discretization of the non-conservative term ( $H\partial R_k/\partial x$ ), the following equation is presented [28]:

$$H \frac{\partial R_g}{\partial x} = HR_g R_l \frac{\partial BG}{\partial x} = HR_g R_l \frac{BG_{i+1} - BG_{i-1}}{2\Delta x} \quad (19)$$

$$H \frac{\partial R_l}{\partial x} = HR_l R_g \frac{\partial BL}{\partial x} = HR_l R_g \frac{BL_{i+1} - BL_{i-1}}{2\Delta x} \quad (20)$$

The derivative  $\partial BG/\partial x$  terms and  $\partial BL/\partial x$  are discretized using centered scheme. The  $BG$  and  $BL$  are presented:

$$BG = \log \left( \frac{R_g}{R_l} \right) \quad (21)$$

$$BL = \log \left( \frac{R_l}{R_g} \right) \quad (22)$$

### Calculation of time step

In order to calculate a time step, at the first,  $\Delta x$  is considered as mesh size, then using the following equation,  $\Delta t$  (*i. e.* time step) is calculated [1]:

$$\Delta t = CFL \frac{\Delta x}{\lambda_{max}^n} \quad (23)$$

In this research, the value of Courant Friedrichs Levy (CFL) number is considered 0.2-0.5. The  $\lambda_{max}^n$  is the maximum value of the wave velocity in solution field at the time  $n$ . Maximum wave velocity for the two-fluid model is equal to the maximum characteristic value of the governing equation in the solution field. The characteristic value of single-pressure two-fluid is presented in Evje and Flatten [10].

### Numerical modelling

In this section, three cases studies (*i. e.* water faucet case, large relative velocity shock pipe case, and Toumi's shock pipe case) are analyzed using the two-fluid model in order to ob-

serve the effect of liquid phase compressibility on the accuracy of the solutions. Accordingly, the first case is a vertical pipe problem and the second and third cases are the horizontal pipe problem.

#### Water faucet case

This system is included a vertical pipe having the height of 12 m and diameter of 1 m. Also, at the initial time, water velocity, air velocity, and volume fraction of water are 10 m/s, 0 and 0.8, respectively, [29]. The water density and air density are 1000 kg/m<sup>3</sup> and 1 kg/m<sup>3</sup>, respectively. The pressure at the outlet of the pipe is 10<sup>5</sup> Pa [29]. The reference and analytical solutions are extracted from Evje and Flatten [24].

In the present study, the single-pressure two-fluid model is considered by the assumption of the liquid phase incompressibility, an incompressible single-pressure model and called (SPM-IC). Also, the single-pressure two-fluid model is considered by the assumption of the liquid phase compressibility, compressible single-pressure model and named (SPM-C).

In order to compare numerical results of the incompressible single-pressure model and compressible single-pressure, pressure changes profile, liquid phase volume fraction profile, gas phase velocity profile, and liquid phase density profile are analyzed. The number of computational mesh, computation time and CFL number are assumed 3200, 0.6 seconds, and 0.5, respectively.

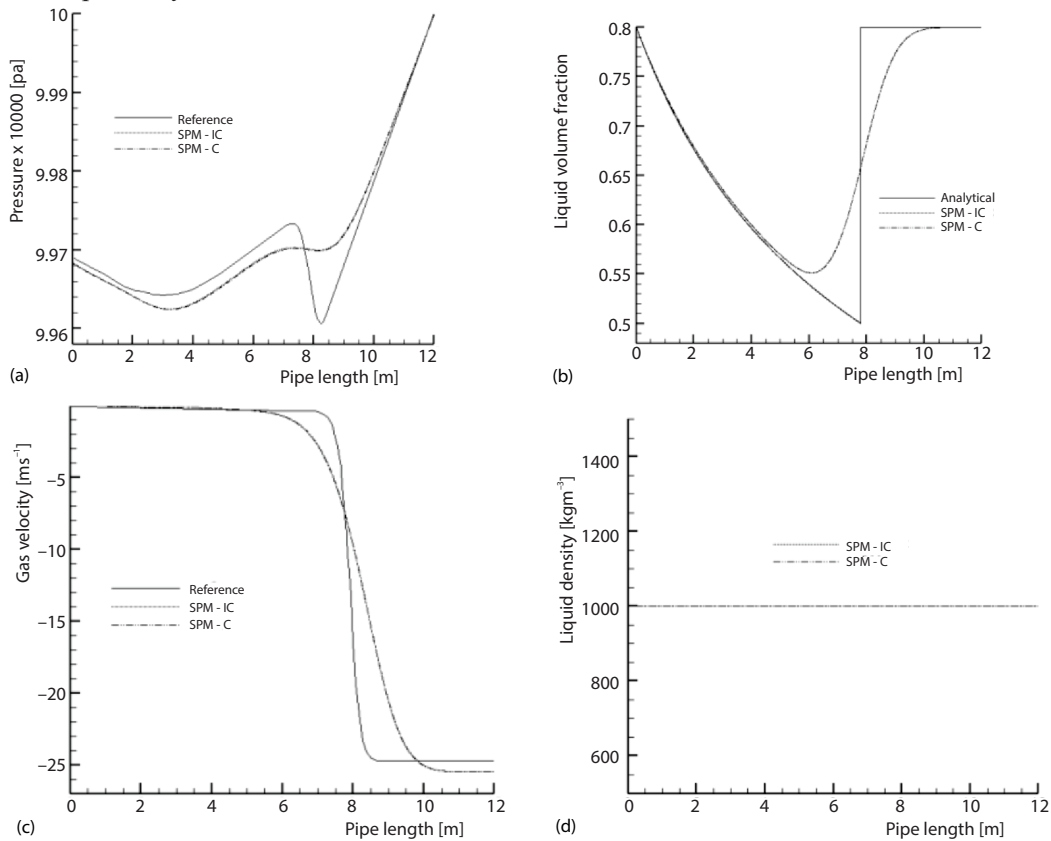


**Figure 1. Water faucet case; comparison incompressible and compressible single-pressure model; (a) pressure, (b) liquid volume fraction, (c) gas velocity, and (d) liquid density**

Figure 1(d) indicates the same results of the liquid phase density changes for the liquid phase density changes for the incompressible single-pressure model and compressible single-pressure. The water faucet case is under atmospheric pressure conditions, and liquid phase density does not change under atmospheric pressure conditions. Due to lack of change in liquid phase density, numerical results are the same for the pressure changes profile, the liquid phase volume fraction profile and the gas phase velocity profile are shown in figs. 1(a)-1(c), respectively. Therefore, in the water faucet case under atmospheric pressure conditions, numerical results of the incompressible single-pressure model and compressible single-pressure are the same.

*Large relative velocity shock pipe case*

This system is included a horizontal pipe having length 100 m and at the 50 m of its length is divided into two part by a diaphragm and it is closed at its two ends. The details of this case and the initial conditions on the left and right sides of the diaphragm are presented in tab. 1 [8]. The reference solution of large relative velocity shock pipe case is obtained from Evje and Flatten [24].

**Table 1. Initial conditions at right and left sides of large relative velocity shock pipe case and Toumi's shock pipe case**

Quantity	Toumi's shock pipe case		Large relative velocity shock pipe case	
	Left	Right	Left	Right
Gas volume fraction	0.25	0.1	0.29	0.3
Liquid velocity [ms <sup>-1</sup> ]	0	0	1	1
Gas velocity [ms <sup>-1</sup> ]	0	0	65	50
Pressure [mpa]	20	10	0.265	0.265
Liquid density [kgm <sup>-3</sup> ]	1000	1000	1000	1000
Gas density [kgm <sup>-3</sup> ]	200	100	2.65	2.65

In order to compare between numerical results of the incompressible single-pressure model and compressible single-pressure model, gas phase density changes profile, liquid phase density changes profile, liquid volume fraction profile and pressure changes profile were calculated. The number of computational mesh, computation time, and Courant Fredrichs Levy number were assumed 1600, 0.1 seconds, and 0.5, respectively.

The initial condition of pressure on large relative velocity shock pipe case is 265000 Pa that is approximately 2.5 times the initial pressure conditions in the water faucet case. Figures 2(a) and 2(b) show results of gas phase density changes profile and liquid phase density changes profile. Increasing pressure (approximately 2.5 times) to the atmospheric pressure in the case of a large relative velocity, in the compressible single-pressure model, leads to compress liquid phase. Therefore, the fig. 2(c) demonstrates the lower growth of liquid phase volume fraction profile in the compressible single-pressure model compared to the incompressible single-pressure model. By compressing the liquid phase, the space required to expand gas phase is created. Therefore, the fig. 2(a) shows the decrease in gas phase density and the fig. 2(b) indicates the increase in liquid phase density in the compressible single-pressure model. As shown in fig. 2(d), pressure change profile in the compressible single-pressure model drops less than it in the incompressible single-pressure model. Numerical results show that, in large relative velocity case, liquid phase compressibility in compressible single-pressure model causes deviation of numerical results relative to the reference solution.

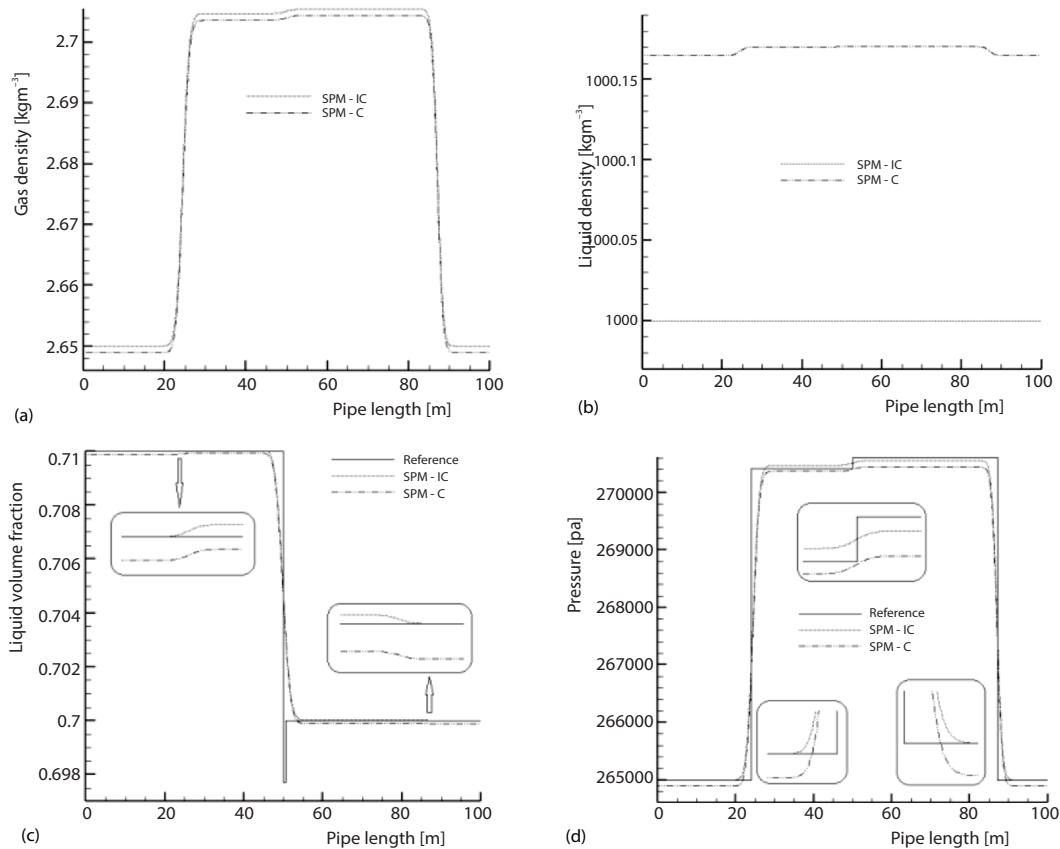


**Figure 2. Large relative velocity shock pipe case; comparison incompressible and compressible single-pressure model; (a) gas density, (b) liquid density, (c) liquid volume fraction, and (d) pressure**

### *Toumi's shock pipe case*

This system is included a horizontal pipe having the length of 100 m and at the length 50 m it is divided into two part by a diaphragm and both ends of the pipe are closed. The reference results of Toumi's shock pipe were obtained from Evje and Flatten [24]. The initial conditions onumi's shock pipe case [30] is presented in the tab. 1.

In order to compare results of the incompressible single-pressure model and compressible single-pressure model, gas phase density changes profile, liquid phase density changes profile, pressure changes profile and gas volume fraction profile were analyzed. The number of computational mesh, computation time and Courant Fredrichs Levy number were assumed 1600, 0.08 seconds, and 0.2, respectively.

In initial conditions of Toumi's shock pipe case, there is a severe pressure gradient on both sides of the diaphragm. Results of phases' density changes profiles are indicated in the figs. 3(a) and 3(b). When there is a severe pressure gradient on both sides of the diaphragm, in the compressible single-pressure model, liquid phase density increases as liquid phase compresses. Due to compressing the liquid phase, this condition is formed to increase the growth of gas phase volume fraction. Results of gas phase volume fraction profile for the incompressible single-pressure model and compressible single-pressure model are indicated in fig. 3(d). In the



numerical modelling, the liquid phase pressure is assumed to be equal to the gas phase pressure. The pressure in the incompressible model, the pressure is calculated using the linear eq. (10). Results presented in fig. 3(c) show that pressure changes profile in the compressible single-pressure model has more drop than the incompressible single-pressure model. The pressure in the compressible model, the pressure is calculated using the linear eq. (12). The eq. (12) is a function of flow variables,  $P = P(\rho_g R_g, \rho_l R_l)$  thus, density changes and volume fraction change of phase influences on the calculation of the term pressure and leads to pressure drop.

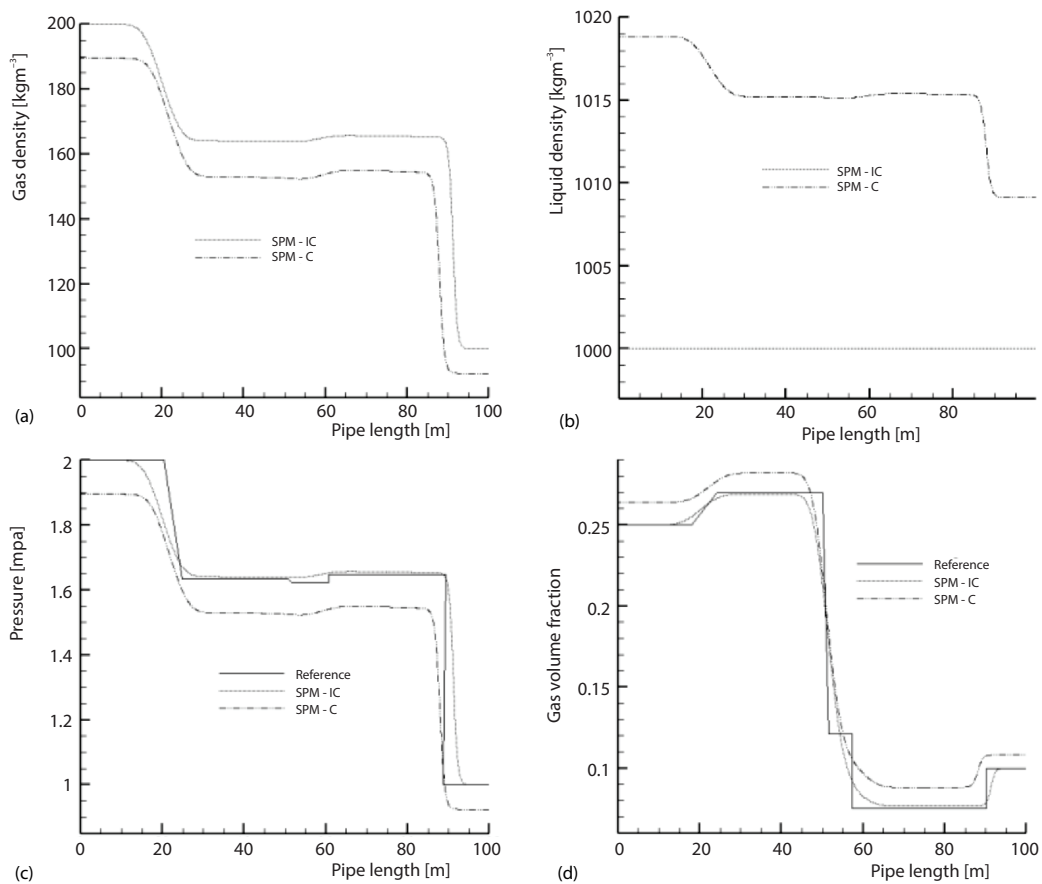


**Figure 3. Toumi's shock pipe case; comparison incompressible and compressible single-pressure model; (a) gas density, (b) liquid density, (c) pressure, and (d) Gas volume fraction**

Since there is a serve pressure gradient in Toumi's shock pipe case, the level of liquid phase density changes was high in the compressible single-pressure model and it was caused deviation of numerical results of the compressible single-pressure model than reference results.

## Conclusion

Governing pressure on the water faucet case is equal to atmospheric pressure and pressure conditions governing on large relative velocity shock pipe case is approximately 2.5 times of the atmospheric pressure. Findings show that in the water faucet case and the large relative velocity shock pipe case, results of the incompressible single-pressure model and compress-

ible single-pressure model are approximately the same. Therefore, if the pressure conditions governing on the case is equal to atmospheric pressure or if it is in the atmospheric pressure range, the liquid phase density changes are not considerable and can be neglected. Numerical results of flow variables show that compressibility of the liquid phase in the compressible single-pressure model causes to the deviation of numerical results to reference results of Toumi's shock pipe case. There is a serve pressure gradient in Toumi's shock pipe case and liquid phase density changes is remarkable. This may cause expansion of gas phase and increase in gas phase volume fraction. By compressing the liquid phase, liquid phase density increases and by compressing the gas phase, gas phase density decreases. According to the eq. (12), the pressure drop in the numerical results of the compressible single-pressure model has resulted from density changes and volume fraction changes of phases in the compressible single-pressure.

## References

- [1] Omgba-Essama, C., Numerical Modelling of Transient Gas-Liquid-Flows (Application Stratified & Slug Flow Regimes), Ph. D. thesis, Cranfield University, Cranfield, UK, 2004
- [2] Ishii, M., *Thermo-Fluid Dynamic Theory of Two-Phase Flow*, Eyrolles, Paris, France, 1975
- [3] Ishii, M., Mishima, K., Two-Fluid Model and Hydrodynamic Constitutive Relations, *Nuclear Engineering and Design*, 82 (1984), 2, pp. 107-126
- [4] Stuhmiller, J., The Influence of Interfacial Pressure Forces on the Character of Two-Phase Flow Model Equations, *International Journal of Multi-Phase Flow*, 3 (1977), 6, pp. 551-560
- [5] Pauchon, C., Banerjee, S., Interphase Momentum Interaction Effects in the Averaged Multifield Model – Part I: Void Propagation in Bubbly Flows, *International Journal of Multi-Phase Flow*, 12 (1986), 4, pp. 559-573
- [6] Ransom, V. H., Hicks, D. L., Hyperbolic Two-Pressure Models for Two-Phase Flow, *Journal of Computational Physics*, 53 (1984), 1, pp. 124-151
- [7] Saurel, R., Abgrall, R., A Multi-Phase Godunov Method for Compressible Multifluid and Multi-Phase Flows, *Journal of Computational Physics*, 150 (1999), 2, pp. 425-467
- [8] Cortes, J., et al., A Density Perturbation Method to Study the Eigenstructure of Two-Phase Flow Equation Systems, *Journal of Computational Physics*, 147 (1998), 2, pp. 463-484
- [9] Song, J. H., Ishii, M., The Well-Posedness of Incompressible 1-D Two-Fluid Model, *International Journal of Heat and Mass Transfer*, 43 (2000), 12, pp. 2221-2231
- [10] Evje, S., Flatten, T., Hybrid Flux-Splitting Schemes for a Common Two-Fluid Model, *Journal of Computational Physics*, 192 (2003), 1, pp. 175-210
- [11] Issa, R., Kempf, M., Simulation of Slug Flow in Horizontal and Nearly Horizontal Pipes with the Two-Fluid Model, *International Journal of Multi-Phase Flow*, 29 (2003), 1, pp. 69-95
- [12] Liao, J., et al., A Study on Numerical Instability of Inviscid Two-Fluid Model Near III-Posedness Condition, *Proceedings*, Proceeding of American Society of Mechanical Engineers, Sun Francisco, Cal., USA, 2005, No. HT2005-72652, pp. 533-541
- [13] Issa, R., et al., Improved Closure Models for Gas Entrainment and Interfacial Shear for Slug Flow Modeling in Horizontal Pipes, *International Journal of Multi-Phase Flow*, 32 (2006), 10, pp. 1287-1293
- [14] Hanyang, G., Liejin, G., Stability of Stratified Gas-Liquid-flow in Horizontal and Near Horizontal Pipes Supported by the National Natural Science Foundation of China (No. 50521604) and Shanghai Jiao Tong University Young Teacher Foundation, *Chinese Journal of Chemical Engineering*, 15 (2007), 5, pp. 619-625
- [15] Ansari, M., Shokri, V., New Algorithm for the Numerical Simulation of Two-Phase Stratified Gas-Liquid-Flow and Its Application for Analyzing the Kelvin-Helmholtz Instability Criterion with Respect to Wavelength Effect, *Nuclear Engineering and Design*, 237 (2007), 24, pp. 2302-2310
- [16] Holmas, H., et al., Analysis of a 1-D Incompressible Two-Fluid Model Including Artificial Diffusion, *IMA Journal of Applied Mathematics*, 73 (2008), 4, pp. 651-667
- [17] Holmas, H., Numerical Simulation of Transient Roll-Waves in Two-Phase Pipe Flow, *Chemical Engineering Science*, 65 (2010), 5, pp. 1811-1825
- [18] Ansari, M., Shokri, V., Numerical Modelling of Slug Flow Initiation in a Horizontal Channels Using a Two-Fluid Model, *International Journal of Heat and Fluid-Flow*, 32 (2011), 1, pp. 145-155
- [19] Ansari, M., Daramizadeh, A., Slug Type Hydrodynamic Instability Analysis Using a Five Equations Hyperbolic Two-Pressure, Two-Fluid Model, *Ocean Engineering*, 52 (2012), Oct., pp. 1-12

- [20] Zeng, Q., et al., Comparison of Implicit and Explicit AUSM-Family Schemes for Compressible Multi-Phase Flows, *International Journal for Numerical Methods in Fluids*, 77 (2015), 1, pp. 43-61
- [21] Shokri, V., Esmaeili, K., Comparison of the Effect of Hydrodynamic and Hydrostatic Models for Pressure Correction Term in Two-Fluid Model in Gas-Liquid Two-Phase Flow Modelling, *Journal of Molecular Liquids*, 237 (2017), July, pp. 334-346
- [22] Paillere, H., et al., On the Extension of the AUSM+ Scheme to Compressible Two-Fluid Models, *Computers and Fluids*, 32 (2003), 6, pp. 891-916
- [23] Li, G., et al., Gas Reservoir Evaluation for Underbalanced Horizontal Drilling, *Thermal Science*, 18 (2014), 5, pp. 1691-1694
- [24] Evje, S., Flatten, T., Hybrid Central-Upwind Schemes for Numerical Resolution of Two-Phase Flows, *ESAIM: Mathematical Modelling and Numerical Analysis*, 39 (2005), 2, pp. 253-273
- [25] Wang, Z., et al., Numerical Simulation of 1-D Two-Phase Flow Using a Pressure-Based Algorithm, *Numerical Heat Transfer – Part A: Applications*, 68 (2015), 4, pp. 369-387
- [26] Toro, E. F., *Riemann Solvers and Numerical Methods for Fluid Dynamics: A Practical Introduction*, Springer Science and Business Media, New York, USA, 2013
- [27] Hirsch, H., *Numerical Computation of Internal and External Flows*, Wiley InterScience, Brussels, Belgium, 1990
- [28] Coquel, F., et al., A Numerical Method Using Upwind Schemes for the Resolution of Two-Phase Flows, *Journal of Computational Physics*, 136 (1997), 2, pp. 272-288
- [29] Ransom, V., Numerical Benchmark Test No. 2. 3: Expulsion of Steam by Sub-Cooled Water, *Multi-Phase Science and Technology*, 3 (1987), 1-4, pp. 124-150
- [30] Toumi, I., An Upwind Numerical Method for Two-Fluid Two-Phase Flow Models, *Nuclear Science and Engineering*, 123 (1996), 2, pp. 147-168